

AD-R148 488

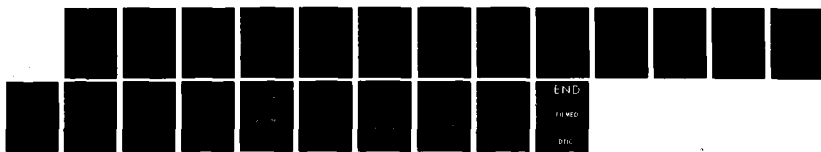
BASIC INSTABILITY MECHANISMS IN CHEMICALLY REACTING
SUBSONIC AND SUPERSONIC. (U) MASSACHUSETTS INST OF TECH
CAMBRIDGE DEPT OF MECHANICAL ENGIN. T Y TOONG

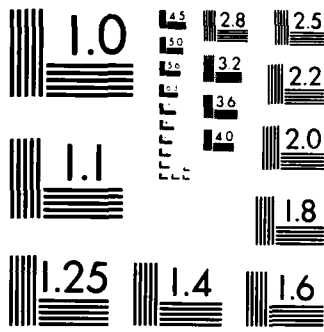
1/1

UNCLASSIFIED

18 OCT 84 AFOSR-TR-84-1115 AFOSR-83-0373 F/G 21/2

NL





MICROCOPY RESOLUTION TEST CHART
NATIONAL BUREAU OF STANDARDS 1963-A

REF ID: A6572
CLASSIFIED

4

DOCUMENTATION PAGE			
1a. REPORT NUMBER AD-A148 408	1b. RESTRICTIVE MARKINGS		
2a. SECURITY CLASSIFICATION SEC. 3	3. DISTRIBUTION/AVAILABILITY OF REPORT Approved for Public Release; Distribution is Unlimited.		
2b. DECLASSIFICATION/DOWNGRADING SCHEDULE			
4. PERFORMING ORGANIZATION REPORT NUMBER(S)	5. MONITORING ORGANIZATION REPORT NUMBER(S) AFOSR-TR-84-1115		
6a. NAME OF PERFORMING ORGANIZATION Massachusetts Inst. of Tech. Dept. of Mechanical Engineering	6b. OFFICE SYMBOL (If applicable)	7a. NAME OF MONITORING ORGANIZATION Same as #8	
6c. ADDRESS (City, State and ZIP Code) Cambridge, MA 02139	7b. ADDRESS (City, State and ZIP Code)		
8a. NAME OF FUNDING/SPONSORING ORGANIZATION AIR FORCE OFFICE OF SCIENTIFIC RESEARCH	8b. OFFICE SYMBOL (If applicable) NA	9. PROCUREMENT INSTRUMENT IDENTIFICATION NUMBER AFOSR-83-0373	
8c. ADDRESS (City, State and ZIP Code) BOLLING AFB DC 20332-6448	10. SOURCE OF FUNDING NOS.		
11. TITLE (Include Security Classification) Basic Instability Mechanisms in Chemically Reacting Subsonic and Supersonic Flows	PROGRAM ELEMENT NO. 61102F	PROJECT NO. 2308	TASK NO. A2
12. PERSONAL AUTHORITY Toong, Tau-Yi	WORK UNIT NO.		
13a. TYPE OF REPORT Annual	13b. TIME COVERED FROM 30/9/83 TO 29/9/84	14. DATE OF REPORT (Yr., Mo., Day) 1984, October, 18	15. PAGE COUNT 21
16. SUPPLEMENTARY NOTATION			

17. COSATI CODES	18. SUBJECT TERMS (Continue on reverse if necessary and identify by block number)		
FIELD	GROUP	SUB GR.	
			Turbulence-Combustion Interactions
			Instability Mechanisms
			Disturbed and Turbulent Flames

19. ABSTRACT (Continue on reverse if necessary and identify by block number)
 Temporal development of spectral changes in the thermal structure of premixed, rod-stabilized, lean methane-air V-flames was examined as a quasi-laminar flame (in the absence of grid-generated turbulence) propagated into the wake region of a neighboring cylindrical rod of different diameters. Significant changes in the spectral structure were observed. In the presence of turbulence-generating grids or disturbance wakes, there was an increase in the intensities of the smaller eddies within the flame brush, thus resulting in higher apparent turbulent-flame-propagation speeds due to rate-augmentation.

Examination of the effects of the equivalence ratio and the turbulence scale and intensity showed the possible role of the coupling between chemical kinetics and turbulence in augmenting the high-frequency fluctuations.

A one-component Laser-Doppler-Velocimetry system was purchased and a traversing mechanism was being constructed.

DTIC FILE COPY

20. DISTRIBUTION/AVAILABILITY OF ABSTRACT UNCLASSIFIED/UNLIMITED <input checked="" type="checkbox"/> SAME AS RPT <input type="checkbox"/> DTIC USERS <input type="checkbox"/>	21. ABSTRACT SECURITY CLASSIFICATION UNCLASSIFIED
22a. NAME OF RESPONSIBLE INDIVIDUAL Julian M Tishkoff	22b. TELEPHONE NUMBER (Include Area Code) (202) 767-4935
	22c. OFFICE SYMBOL AFOSR/ NA E

DTIC
ELECTRONIC
DEC 10 1984

AFOSR-TR-34-1115



Accession For	NTIS GRA&I	X
DTIC TAB	Unannounced	<input type="checkbox"/>
Justification		
By _____	Distribution/	
Availability Codes		
Av. Reprod/	Int'l. Reprod/	
A-1		

ANNUAL TECHNICAL REPORT ON RESEARCH

SUPPORTED BY GRANT AFOSR-83-0373

(September 30, 1983-September 29, 1984)

Basic Instability Mechanisms
in Chemically Reacting Subsonic and Supersonic Flows

Tau-Yi Toong

Massachusetts Institute of Technology

Summary of Progress

Temporal development of spectral changes in the thermal structure of premixed, rod-stabilized, lean methane-air V-flames was examined as a quasi-laminar flame (in the absence of grid-generated turbulence) propagated into the wake region of a neighboring cylindrical rod of different diameters. Significant changes in the spectral structure were observed. In the presence of turbulence-generating grids or disturbance wakes, there was an increase in the intensities of the smaller eddies within the flame brush, thus resulting in higher apparent turbulent-flame-propagation speeds due to rate-augmentation.

Examination of the effects of the equivalence ratio and the turbulence scale and intensity showed the possible role of the coupling between chemical kinetics and turbulence in augmenting the high-frequency fluctuations.

A one-component Laser-Doppler-Velocimetry system was purchased and a traversing mechanism was being constructed.

Approved for public release;
distribution unlimited.

84 12 03 227

I. Objective and Scope of Work

The main objective of this research is to determine and elucidate the mechanisms governing turbulence-combustion interactions in different spectral regimes. During the past grant period, temporal development of spectral changes in the thermal structure of premixed, rod-stabilized, lean methane-air V-flames was examined as a quasi-laminar flame propagated into the wake region of a neighboring cylinder. Significant changes in the spectral structure were observed. In the presence of turbulence-generating grids or disturbance wakes, there was an increase in the intensities of the smaller eddies within the flame brush, thus resulting in higher apparent turbulent-flame-propagation speeds due to rate-augmentation.

A one-component Laser-Doppler-Velocimetry (LDV) system was purchased from TSI with the support of a DoD-University Research Instrumentation Grant. A traversing mechanism was designed and being constructed.

II. Results and Discussion

Detailed spectral changes in the structure of disturbed and undisturbed flames were examined by measuring instantaneous temperatures within the flame brush by the use of frequency-compensated, 25 μm -diameter, Pt/Pt-10% Rh thermocouples. Simultaneous velocity fluctuations upstream of the flames were also measured by means of a hot-wire anemometer. The results obtained are briefly described below.

(1) Spectral Density Distributions

In order to elucidate the mechanisms governing turbulence-combustion interactions, temporal development of spectral changes in the thermal structure of premixed, rod-stabilized, lean methane-air V-flames was examined as a quasi-laminar flame (in the absence of grid-generated turbulence) propagated into the wake region of a neighboring cylindrical rod of four different diameters (1.6, 0.89, 0.64 and 0.41 mm). Spectral density distributions of apparent all-pass mean-square temperature fluctuations within disturbed flames were compared with those within undisturbed and turbulent flames (in the presence of turbulence-generating grids of corresponding mesh size) at different distances downstream from the cylindrical flameholder.

Figure 1 shows comparisons of the spectral density distributions* within undisturbed, disturbed and turbulent flames at 3 and 35 mm downstream from the flameholder. The diameter of the disturbance rod in this case was 1.6 mm, the same as that of the 4-mesh turbulence-generating grid in the study of turbulent flames. (This disturbed flame was thus designated as DF4.) The temperature fluctuations were monitored at a position within the flame brush where the apparent all-pass RMS temperature fluctuations were the maximum. (Other conditions were specified in the caption.) Note that at 3 mm downstream (cf. Fig. 1a), the spectral structure within the disturbed flame resembled that within the undisturbed flame (UDF), while at 35 mm downstream (cf. Fig. 1b), the structure of

* Integrated area under the curve between two specific frequencies represents the mean-square temperature fluctuations within the band pass.

DF4 approached that of the corresponding turbulent flame (TF4), thus showing the temporal development of the disturbance effect from the neighboring cylinder. Note also that the structure within the undisturbed flame showed a peak at approximately 200 Hz, which corresponded to the predominant frequency observed in the velocity fluctuations along the centerline of the 2.1 mm-diameter flameholder in the absence of the flame.

Figure 2 shows comparisons of the spectral density distributions within undisturbed, disturbed (DF10) and turbulent flames (TF10) at 3 and 35 mm downstream of the flameholder. Here, the diameter of the disturbance rod was reduced to 0.64 mm, which corresponded to the rod diameter in a 10-mesh grid used in the study of TF10. With the smaller disturbance rod, the spectral structure of DF10 resembled that of UDF even at 35 mm downstream. Unlike DF4, the structure of which approached that of TF4 at 35 mm downstream, the spectral densities within DF10 remained lower than those within TF10 in the presence of a 10-mesh grid. Furthermore, in the presence of the lower turbulence intensities and smaller scales, both DF10 and TF10 still showed peaks in the spectral densities at \sim 200 Hz (characteristic of the undisturbed flame) at 35 mm downstream.

Figure 3 shows comparisons of the spectral density distributions at 3 and 35 mm downstream of the flameholder in the presence of disturbance rods of different diameters. At 3 mm downstream, DF4, 6 and 10 seemed to give nearly the same structure in the high-frequency region. Farther downstream at 35 mm downstream, on the other hand, DF4 (in the presence of the largest disturbance rod) showed the highest spectral densities while DF10 and 20 gave nearly the same structure and DF6 (in the presence of a

disturbance rod of an intermediate diameter) began to show some deviation in a limited spectral regime. These observations seem to imply that the effects of the disturbance rods on the spectral structure are due to interactions of rate processes which become more pronounced with increasing time as the flow moves downstream.

Figure 4 shows the development of the spectral density distributions within disturbed flames, DF4 and DF10, at increasing distance downstream from the flameholder. As noted earlier in Fig. 1, the structure of DF4 (cf. Fig. 4a) changed from one characteristic of the undisturbed flame to one characteristic of the corresponding turbulent flame. On the other hand, the structure of DF10 (cf. Fig. 4b) seemed to retain the characteristic of the undisturbed flame with peak spectral density at ~ 200 Hz. It would be of great interest to investigate the temporal development of these structures in order to shed light on the mechanisms governing the turbulence-combustion interactions leading to such changes.

(2) High-Frequency Fluctuations

Due to the presence of low-frequency fluctuations which would lead to slow drifting of the flame across the temperature-monitoring station, the long-time signals obtained at a given spatial position in the laboratory-reference coordinates did not originate from a fixed position within the flame brush. In order to shed light on the nature of the higher-frequency components at different "instantaneous" mean temperatures within the flame brush, the signals should be analyzed within time intervals much shorter than the characteristic time of the low-frequency fluctuations. One can then relate these fluctuations to the chemical effect at a mean temperature

pertaining to this time interval and the corresponding reaction rate and infer therefrom whether they are due to possible coupling between chemical kinetics and turbulence on the basis of our understanding of the instability mechanisms in reacting flows.

(a) Effect of Equivalence Ratio

Figure 5 shows comparisons of the RMS temperature fluctuations within the high-frequency region at different "instantaneous" mean temperatures (pertaining to a time interval of 25 ms^{*}) for a turbulent flame TF4 (with 4-mesh grid) and an undisturbed quasi-laminar flame (without grid-generated turbulence) at two equivalence ratios, 0.75 and 0.85, and at 35 mm downstream of the flameholder. Despite some scatter, Fig. 5 shows that the RMS temperature fluctuations were the highest within the reaction zone and lower near the unburned and the burned regions, thus implying the possible role of chemical reaction rate in augmenting the higher-frequency fluctuations. This implication was further substantiated by the effect of the equivalence ratio on the high-frequency fluctuations for both TF4 and UDF. (Note that at the same mean temperature, the RMS values were significantly higher at the higher equivalence ratio.) Consistent with the comparison of the spectral density distributions of apparent all-pass mean-square temperature fluctuations (shown in Fig. 1), the RMS values were also higher for the turbulent flame at the same mean temperature and equivalence ratio.

* A characteristic time of the observed low-frequency fluctuations was about 200 ms.

(b) Effect of Disturbance Wake

Temporal development of the RMS temperature fluctuations within the high-frequency region was examined for undisturbed, disturbed and turbulent flames. Figure 6 shows comparisons at 3 and 35 mm downstream of the flameholder. Consistent with the spectral density distributions shown in Fig. 1, the RMS values for DF4 were nearly the same as those for UDF at 3 mm downstream (cf. Fig. 6a). On the other hand, at 35 mm downstream, the RMS values for DF4 were much higher than those for TF4 (cf. Fig. 6b). Again, one notes that the RMS values were higher within the reaction zone.

The effect of disturbance rods of different diameters on the high-frequency fluctuations was also examined. Figure 7 shows comparisons at 10, 15 and 25 mm downstream for the disturbed flames, DF4 and DF6. Consistent with Fig. 3, the high-frequency fluctuations were augmented to higher values in the presence of the larger disturbance rod, thus implying that the relevant interactions leading to the augmentation might also depend on the intensities and scales of turbulence generated by the disturbance rods. Coupled with the earlier observation on the chemical effect at different mean temperatures and equivalence ratios, one can expect that the interactions governing the augmentation of the high-frequency fluctuations may depend on the coupling between chemical kinetics and turbulence.

Temporal development of the turbulence-combustion interactions with increasing distance downstream was further demonstrated in Fig. 8 for DF6 and DF4. The question is whether examination of such development can lead to an understanding of the governing mechanism. Work is in progress to attempt to answer this question.

(3) Low-Frequency Fluctuations

Analysis of the high-frequency components within time intervals much shorter than the characteristic time of the low-frequency fluctuations suggested that the mechanism governing the augmentation of the high-frequency fluctuations may depend on the coupling between chemical kinetics and turbulence. The "instantaneous" mean temperatures obtained in this analysis were found to fluctuate at rather low frequencies. Preliminary examination showed that these low-frequency fluctuations might also be related to the "apparent" mean temperature pertaining to a time interval longer than their characteristic time.

(4) Velocity Field

In order to elucidate the mechanism governing the low-frequency fluctuations, work has begun to monitor simultaneously the temperature fluctuations within the disturbed, the undisturbed and the turbulent flames by means of fine-wire thermocouples and the velocity fluctuations upstream of the flames by means of a hot-wire anemometer. The objective of these experiments is to examine whether the presence of a flame can trigger and amplify instabilities in the flow field upstream.

Preliminary results appeared to show the development of low-frequency fluctuations in the velocity field in the presence of a quasi-laminar flame. They also showed the effect of the shear layer between the mixture flow and the ambient on the flame structure at about 50 mm downstream of the flameholder and beyond. Further work in progress should include the control of this layer by means of a secondary air flow surrounding the burner.

In order to further understand the mechanisms governing turbulence-combustion interactions in different spectral regimes, experiments are planned to examine simultaneous temperature and velocity fluctuations within the flame brush. A one-component LDV system was purchased recently from TSI and the necessary traversing mechanism is now under construction.

III. Publications and Reports

See attached Enclosure I.

IV. Professional Personnel

Professor T. Y. Toong and Dr. G. E. Abouseif.

V. Interactions

A seminar on Turbulence-Combustion Interactions was presented by T. Y. Toong at the Massachusetts Institute of Technology on April 26, 1984.

CAPTION TO FIGURES

- Figure 1: Comparisons of spectral density distributions of apparent all-pass mean-square temperature fluctuations within undisturbed (UDF), disturbed (DF4 with 1.6 mm-diameter disturbance rod) and turbulent (TF4 with 4-mesh grid) flames at a position of maximum apparent all-pass RMS temperature fluctuations; equivalence ratio, 0.75; mean mixture velocity, 2.4 m/s; (a) 3 mm downstream of 2.1 mm-diameter flameholder (b) 35 mm downstream
- Figure 2: Comparisons of spectral density distributions of apparent all-pass mean-square temperature fluctuations within undisturbed (UDF), disturbed (DF10 with 0.64 mm-diameter disturbance rod) and turbulent (TF10 with 10-mesh grid) flames at a position of maximum apparent all-pass RMS temperature fluctuations; equivalence ratio, 0.75; mean mixture velocity, 2.4 m/s; (a) 3 mm downstream of 2.1 mm-diameter flameholder (b) 35 mm downstream
- Figure 3: Comparisons of spectral density distributions of apparent all-pass mean-square temperature fluctuations within disturbed flames, DF4 (with 1.6 mm-diameter disturbance rod), DF6 (0.89 mm-diameter), DF10 (0.64 mm-diameter) and DF 20 (0.41 mm-diameter), at a position of maximum apparent all-pass RMS temperature fluctuations; equivalence ratio, 0.75; mean mixture velocity, 2.4 m/s; (a) 3 mm downstream of 2.1 mm-diameter flameholder (b) 35 mm downstream
- Figure 4: Comparisons of spectral density distributions of apparent all-pass mean-square temperature fluctuations at different distances downstream of 2.1 mm-diameter flameholder at a position of maximum apparent all-pass RMS temperature fluctuations; equivalence ratio, 0.75; mean mixture velocity, 2.4 m/s; (a) disturbed flame DF4 with 1.6 mm-diameter disturbance rod (b) disturbed flame DF10 with 0.64 mm-diameter disturbance rod
- Figure 5: Comparisons of RMS temperature fluctuations within high-frequency region at different "instantaneous" mean temperatures (pertaining to a time interval of 25 ms) for two equivalence ratios ($\phi = 0.85$ and 0.75) at a position of maximum apparent all-pass RMS temperature fluctuations 35 mm downstream of 2.1 mm-diameter flameholder; mean mixture velocity, 2.4 m/s; (a) quasi-laminar flame, without grid-generated turbulence (b) turbulent flame with 4-mesh grid

Figure 6: Comparisons of RMS temperature fluctuations within high-frequency region at different "instantaneous" mean temperatures (pertaining to a time interval of 25 ms) for undisturbed UDF, disturbed DF4 (with 1.6 mm-diameter disturbance rod) and turbulent TF4 (with 4-mesh grid) at a position of maximum apparent all-pass RMS temperature fluctuations; equivalence ratio, 0.75; mean mixture velocity, 2.4 m/s; (a) 3 mm downstream of 2.1 mm-diameter flameholder (b) 35 mm downstream

Figure 7: Comparisons of RMS temperature fluctuations within high-frequency region at different "instantaneous" mean temperatures (pertaining to a time interval of 25 ms) for disturbed flames DF4 (with 1.6 mm-diameter disturbance rod) and DF6 (0.89 mm-diameter) at a position of maximum apparent all-pass RMS temperature fluctuations; equivalence ratio, 0.75; mean mixture velocity, 2.4 m/s; (a) 10 mm downstream of 2.1 mm-diameter flameholder (b) 15 mm downstream (c) 25 mm downstream

Figure 8: Comparisons of RMS temperature fluctuations within high-frequency region at different "instantaneous" mean temperatures (pertaining to a time interval of 25 ms) at different distances downstream of 2.1 mm-diameter flameholder at a position of maximum apparent all-pass RMS temperature fluctuations; equivalence ratio, 0.75; mean mixture velocity, 2.4 m/s; (a) disturbed flame DF6 with 0.89 mm-diameter disturbance rod (b) disturbed flame DF4 with 1.6 mm-diameter disturbance rod

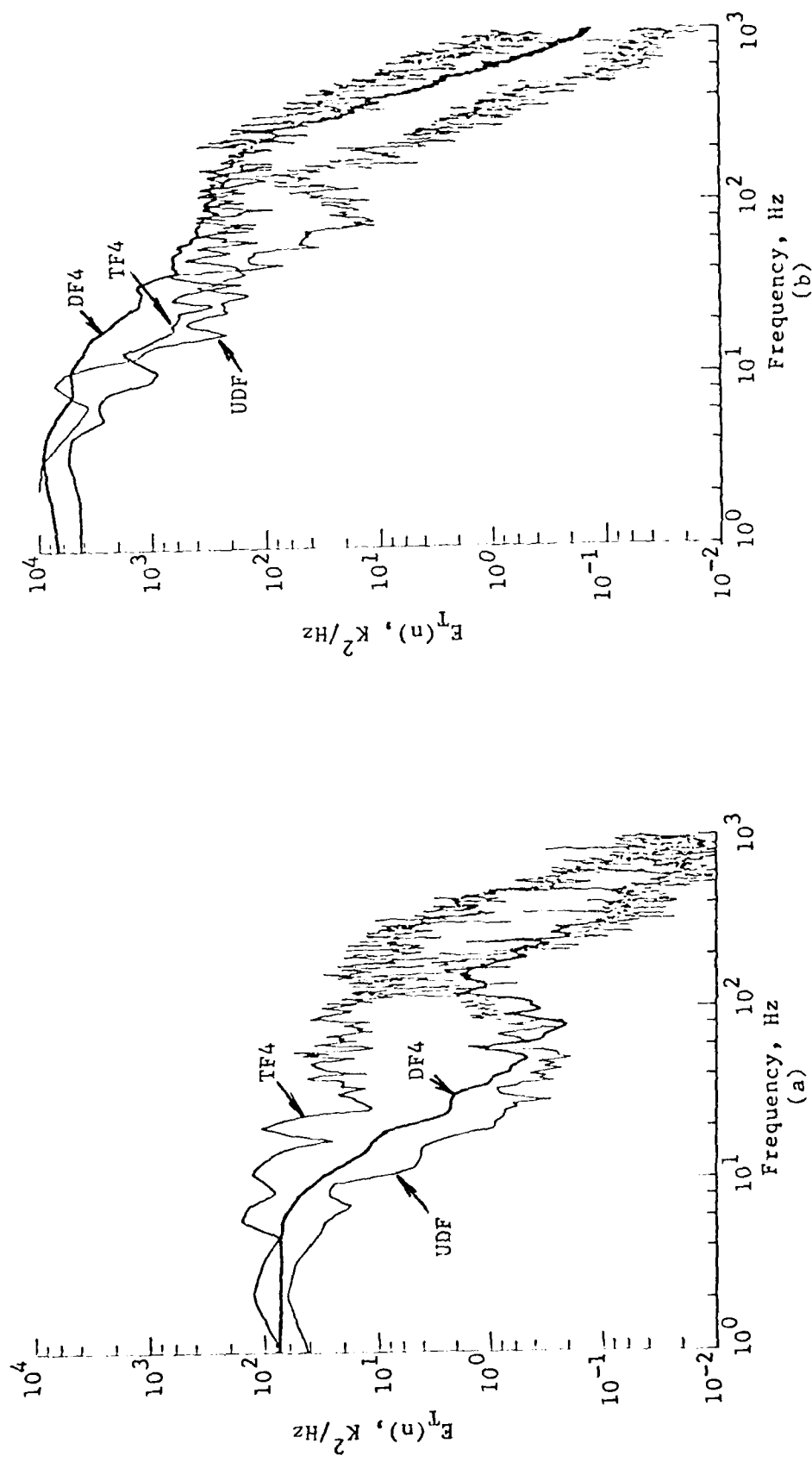


Fig. 1 Comparisons of spectral density distributions of apparent all-pass mean-square temperature fluctuations within undisturbed (UDF), disturbed (DF4 with 1.6 mm-diameter disturbance rod) and turbulent (TF4 with 4-mesh grid) flames at a position of maximum apparent all-pass RMS temperature fluctuations; equivalence ratio, 0.75; mean mixture velocity, 2.4 m/s; (a) 3 mm downstream of 2.1 mm-diameter flameholder (b) 35 mm downstream

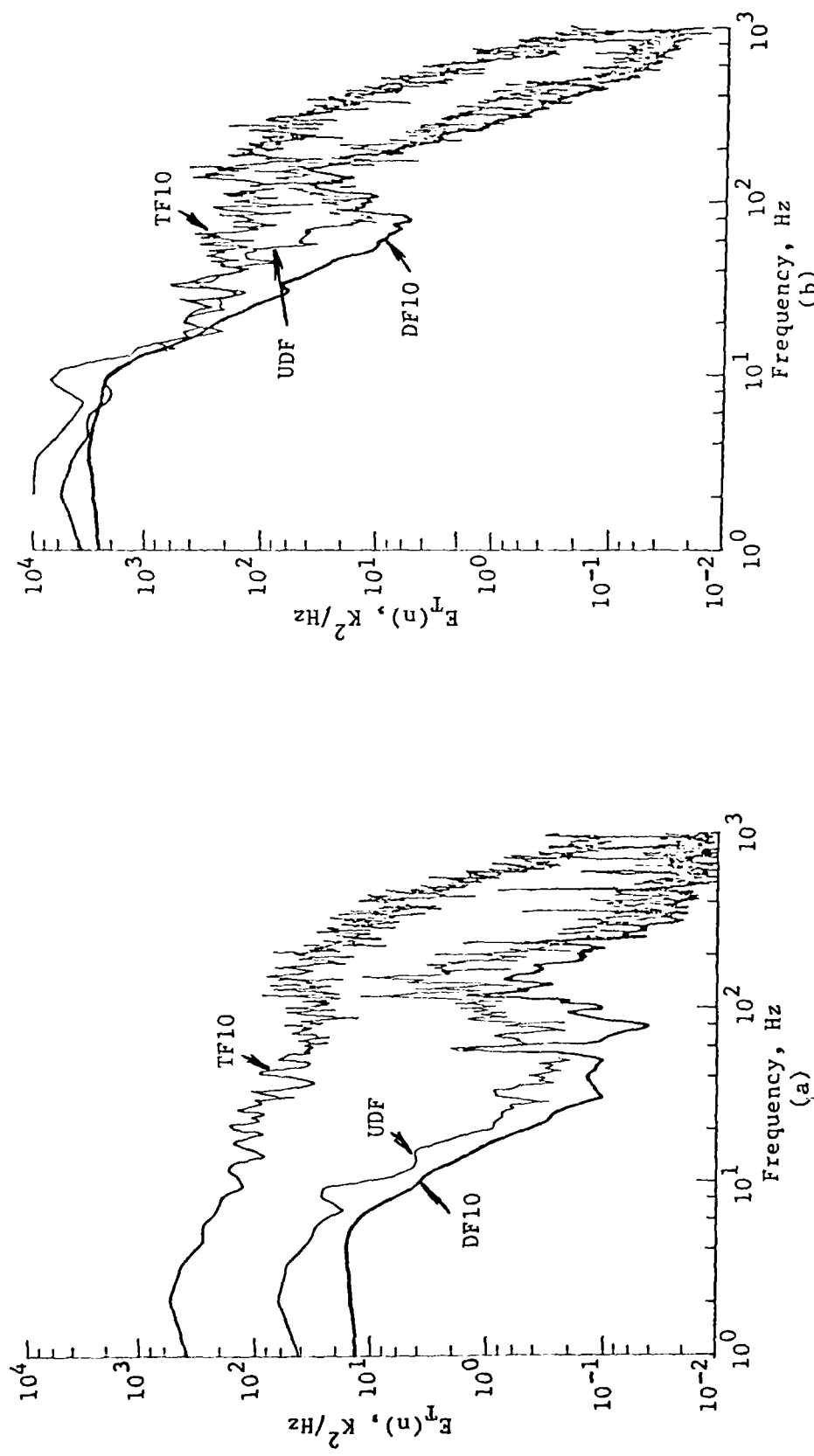


Fig. 2 Comparisons of spectral density distributions of apparent all-pass mean-square temperature fluctuations within undisturbed (UDF), disturbed (DF10 with 0.64 mm-diameter disturbance rod) and turbulent (TF10 with 1D-mesh grid) flames at a position of maximum apparent all-pass RMS temperature fluctuations; equivalence ratio, 0.75; mean mixture velocity, 2.4 m/s; (a) 3 mm downstream of 2.1 mm-diameter flameholder (b) 35 mm downstream

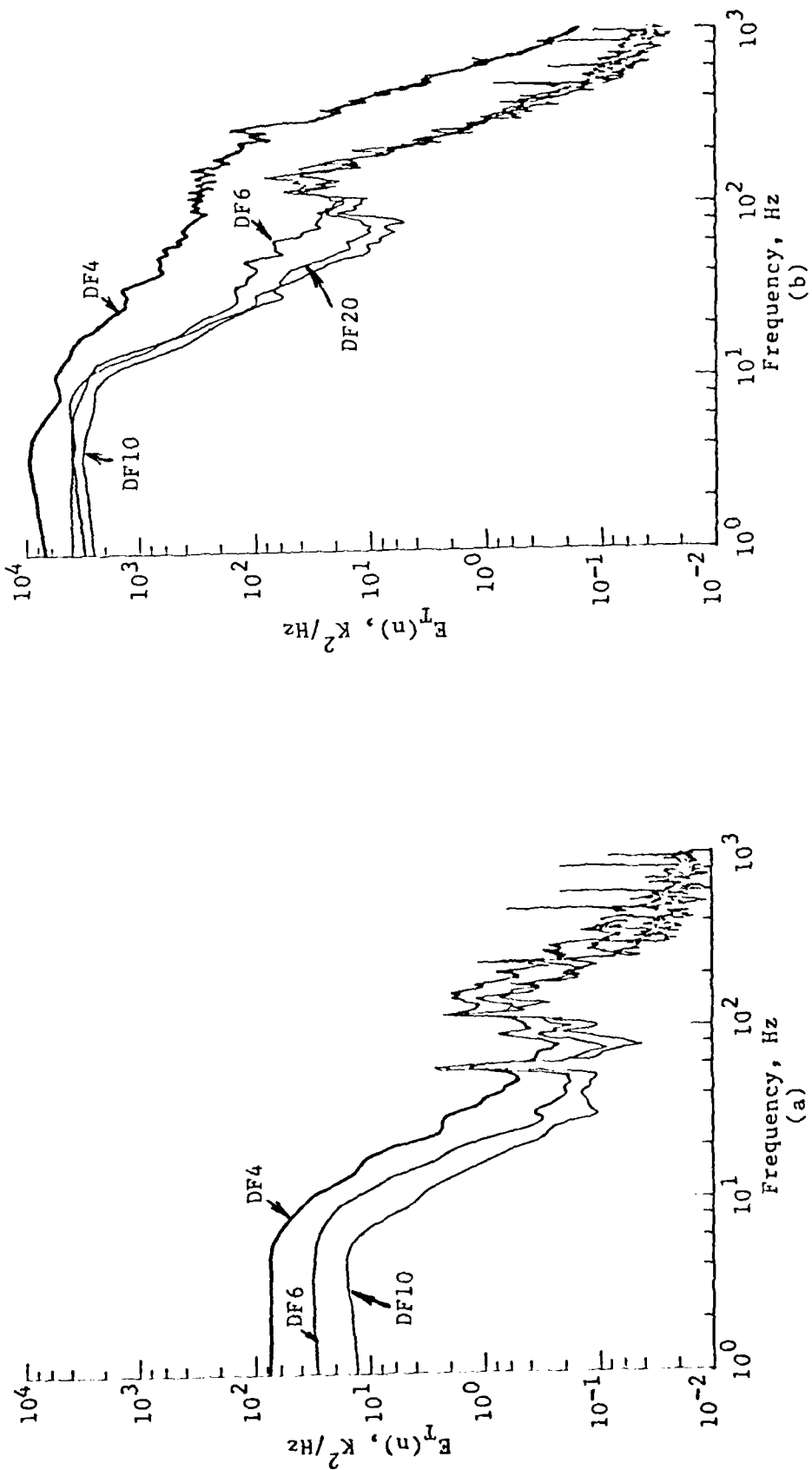


Fig. 3 Comparisons of spectral density distributions of apparent all-pass mean-square temperature fluctuations within disturbed flames, DF4 (with 1.6 mm-diameter disturbance rod), DF6 (0.89 mm-diameter), DF10 (0.64 mm-diameter) and DF20 (0.41 mm-diameter), at a position of maximum apparent all-pass RMS temperature fluctuations; equivalence ratio, 0.75; mean mixture velocity, 2.4 m/s; (a) 3 mm downstream of 2.1 mm-diameter flameholder (b) 35 mm downstream

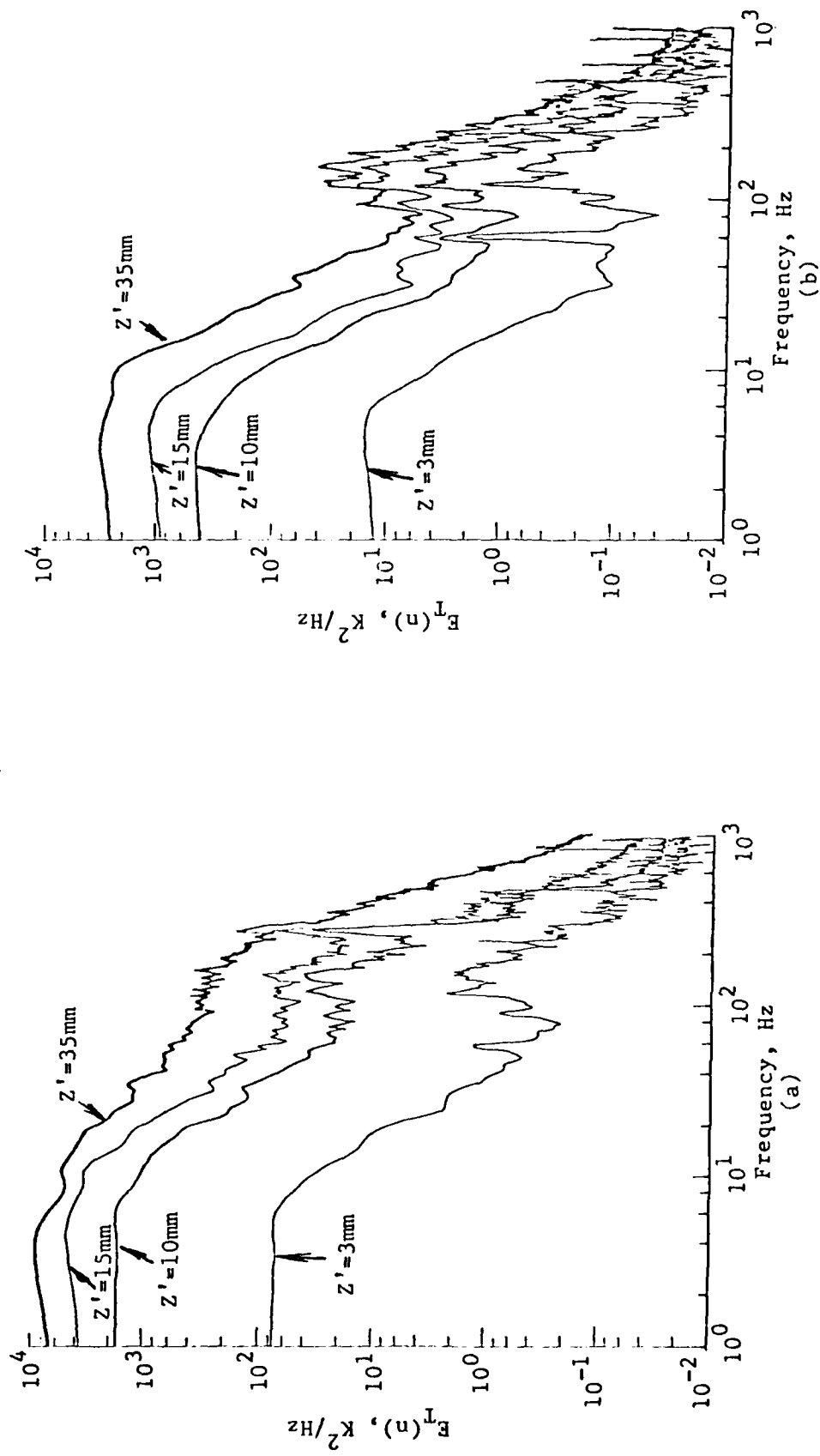


Fig. 4 Comparisons of spectral density distributions of apparent all-pass mean-square temperature fluctuations at different distances downstream of 2.1 mm-diameter flameholder at a position of maximum apparent all-pass RMS temperature fluctuations; equivalence ratio, 0.75; mean mixture velocity, 2.4 m/s; (a) disturbed flame DF4 with 1.6 mm-diameter disturbance rod (b) disturbed flame DF10 with 0.64 mm-diameter disturbance rod

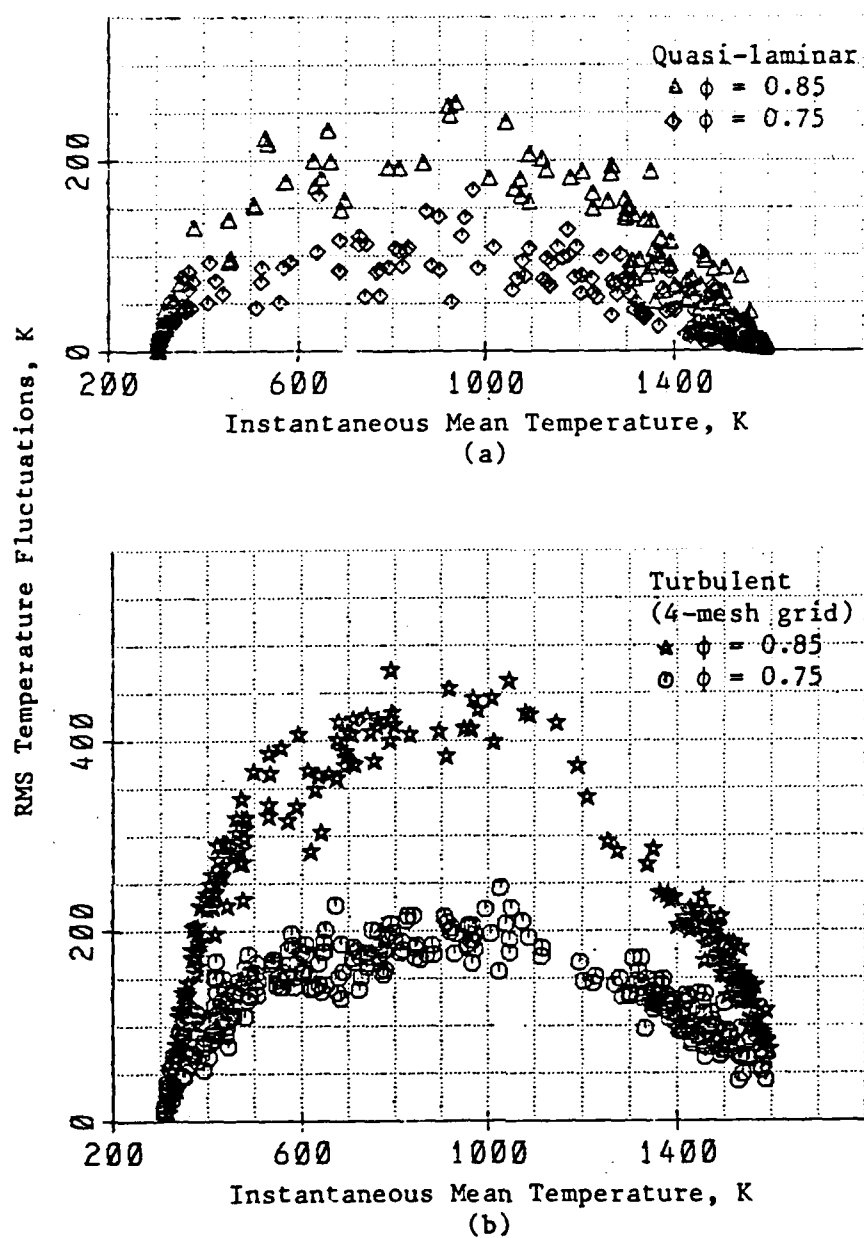


Fig. 5 Comparisons of RMS temperature fluctuations within high-frequency region at different "instantaneous" mean temperatures (pertaining to a time interval of 25 ms) for two equivalence ratios ($\phi = 0.85$ and 0.75) at a position of maximum apparent all-pass RMS temperature fluctuations 35 mm downstream of 2.1 mm-diameter flameholder; mean mixture velocity, 2.4 m/s; (a) quasi-laminar flame, without grid-generated turbulence (b) turbulent flame with 4-mesh grid

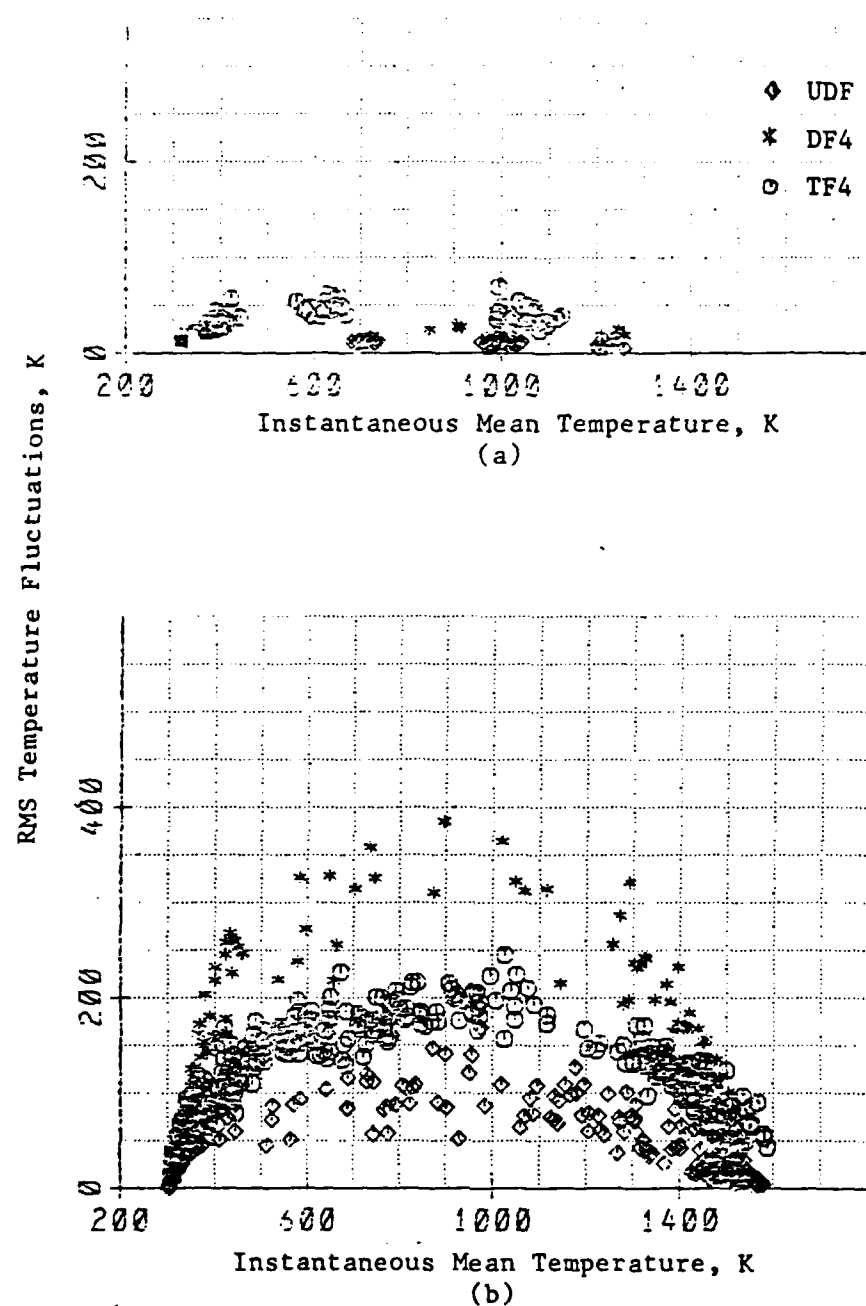


Fig. 6 Comparisons of RMS temperature fluctuations within high-frequency region at different "instantaneous" mean temperatures (pertaining to a time interval of 25 ms) for undisturbed UDF, disturbed DF4 (with 1.6 mm-diameter disturbance rod) and turbulent TF4 (with 4-mesh grid) at a position of maximum apparent all-pass RMS temperature fluctuations; equivalence ratio, 0.75; mean mixture velocity, 2.4 m/s; (a) 3 mm downstream of 2.1 mm-diameter flameholder (b) 35 mm downstream

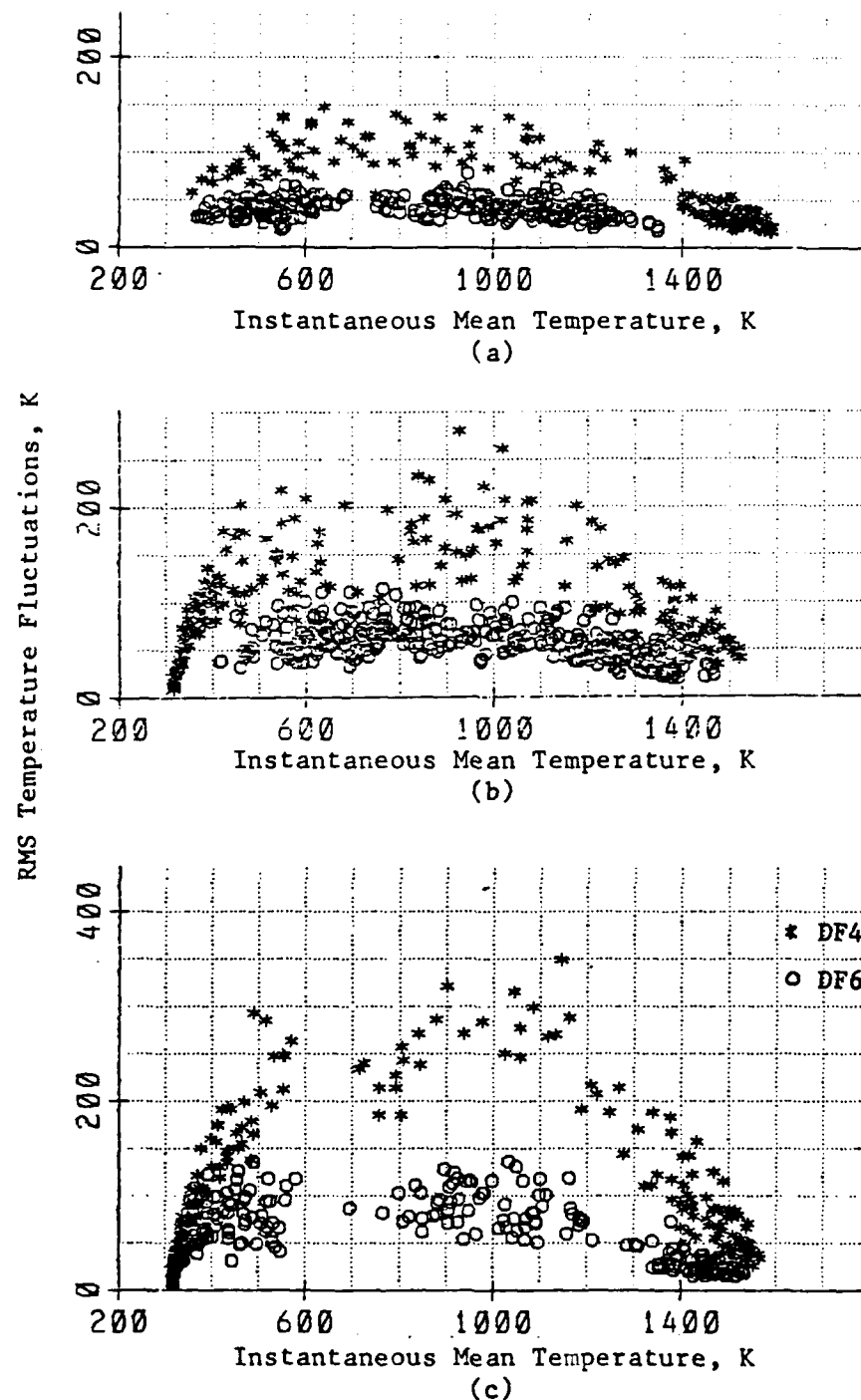


Fig. 7 Comparisons of RMS temperature fluctuations within high-frequency region at different "instantaneous" mean temperatures (pertaining to a time interval of 25 ms) for disturbed flames DF4 (with 1.6 mm-diameter disturbance rod) and DF6 (0.89 mm-diameter) at a position of maximum apparent all-pass RMS temperature fluctuations; equivalence ratio, 0.75; mean mixture velocity, 2.4 m/s; (a) 10 mm downstream of 2.1 mm-diameter flameholder (b) 15 mm downstream (c) 25 mm downstream

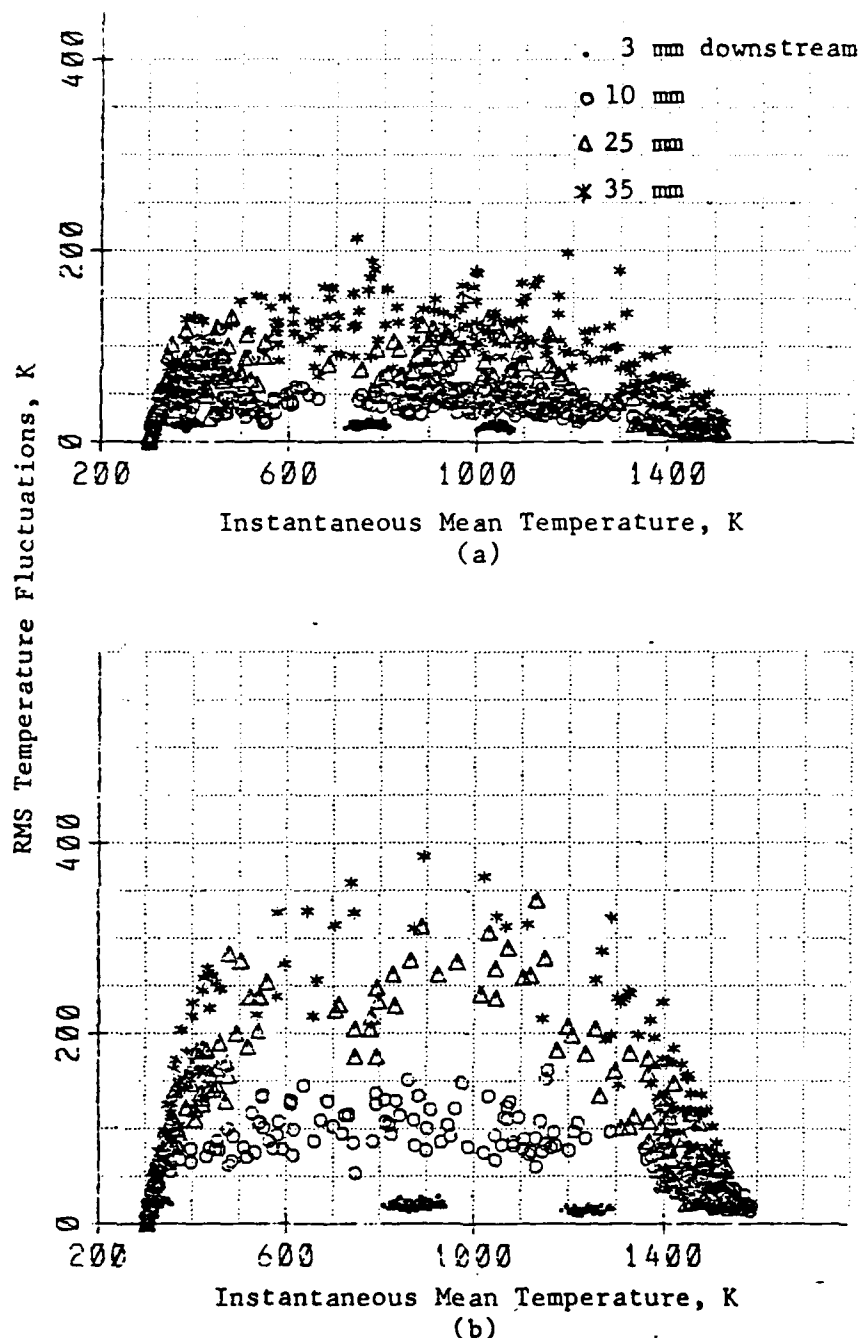


Fig. 8 Comparisons of RMS temperature fluctuations within high-frequency region at different "instantaneous" mean temperatures (pertaining to a time interval of 25 ms) at different distances downstream of 2.1 mm-diameter flameholder at a position of maximum apparent all-pass RMS temperature fluctuations; equivalence ratio, 0.75; mean mixture velocity, 2.4 m/s; (a) disturbed flame DF6 with 0.89 mm-diameter disturbance rod (b) disturbed flame L4 with 1.6 mm-diameter disturbance rod

ENCLOSURE I

**Basic Instability Mechanisms
in Chemically Reacting Subsonic and Supersonic Flows**

**Publications and Reports
(Grant AFOSR-83-0373)**

1. Abouseif, G. E., Keklak, J. A. and Toong, T. Y., "Ramjet Rumble:
The Low-Frequency Instability Mechanism in Coaxial Dump Combustors",
Combustion Science and Technology, 36, pp. 83-108, 1984.

2. Abouseif, G. E. and Toong, T. Y., "Theory of Unstable Two-Dimensional
Detonations: Genesis of Transverse Waves", to be submitted for
publication in Combustion and Flame.

END

FILMED

1-85

DTIC